Title: Stroke-Related Changes in Tonic and Phasic Muscle Recruitment During Reaching Reveal Pathway-Specific Motor Deficits

Anna S. Korol (ak00028@mix.wvu.edu), Amelia Adcock (akadcock@hsc.wvu.edu), and Valeriya Gritsenko (vgritsenko@mix.wvu.edu)

Affiliations: West Virginia University, Morgantown, WV

Key words: Upper limb, motor control, electromyography, intersegmental dynamics, gravity, posture, corticospinal tract, reticulospinal tract, principal component analysis, motor impairment assessment, neuromechanics, biomechanics

Abstract

Background and Purpose: Upper limb motor deficits are common after stroke and often persist despite rehabilitation. Clinical assessments focus on movement quality but fail to quantify underlying neuromuscular impairments, especially in individuals with mild deficits. We aimed to characterize stroke-related changes in muscle recruitment during reaching by separating tonic (gravity-compensating) and phasic (intersegmental dynamics-related) components of electromyographic (EMG) activity and assessing their relationship to motor impairment.

Methods: In this cross-sectional study, we recorded surface EMG from 12 upper limb muscles during goal-directed reaching in 8 participants with unilateral ischemic stroke and 9 age-matched controls. Using principal component analysis, we extracted tonic and phasic components of muscle activity and compared their amplitude, directional tuning, and coactivation patterns across groups. Score differences between stroke and control groups were analyzed using generalized linear mixed-effects models, regression analyses, and correlation with time since stroke and previously published muscle torque-based performance indices.

Results: Individuals with stroke exhibited disrupted muscle recruitment even with mild motor deficits. Proximal muscles were over-recruited in directions that normally require less muscle activation, indicating abnormal directional tuning. Phasic activation of distal muscles was significantly reduced and declined further with time post-stroke (R^2 = 0.52, p = 0.002), while tonic overactivation of proximal muscles was present in all participants with stroke. Coactivation between multiple muscles was altered, with right-hemisphere stroke reducing tonic coactivation in contralateral arms and left-hemisphere

stroke increasing it. Abnormal phasic coactivation between proximal and distal muscles was present and correlated with impaired limb propulsion ($R^2 = 0.67$, $p = 0.013$). Tonic and phasic recruitment deficits were often correlated, suggesting shared disruption of corticospinal and reticulospinal pathways.

Conclusions: Stroke causes distinct yet interacting impairments in tonic and phasic muscle recruitment that underlie individual motor deficits. These findings support the need for neuromechanically informed assessment tools that target specific motor pathways to guide individualized rehabilitation strategies.

Introduction

Stroke is the third leading cause of combined mortality and disability worldwide [1], with upper limb motor impairment affecting 80% of survivors [2] only half of whom regain useful upper limb function.[3] Despite advances in rehabilitation, many individuals continue to experience poor arm control even years after stroke onset. Clinical assessments often focus on observable movement quality or joint angles, which cannot assess fatigue and may overlook the underlying neuromuscular coordination strategies that shape recovery.[4] Understanding how stroke alters the recruitment of specific muscle groups, especially in response to biomechanical demands such as antigravity support and intersegmental dynamics, is essential for developing more targeted individualized rehabilitation strategies.[5,6]

Clinical assessments often rely on low-resolution scoring systems and extensive rater training to address subject and observer variability. While this approach improves consistency, it reduces responsiveness and predictive validity—particularly in patients with mild motor deficits—by introducing ceiling effects.[7,8] These tests also fail to differentiate impairments caused by passive mechanics from those due to active muscle coordination. As a result, treatments developed using these assessments show inconsistent effectiveness in randomized clinical trials.[9–11] We have previously demonstrated the utility of objective motion capture for assessing complex arm impairments after stroke and shoulder deficits following chest surgery.[12,13] We also showed that measuring muscle torques from motion capture offers a more sensitive measure of post-stroke motor deficits than that based on joint angles.[14] This approach is particularly valuable for patients with minimal visible impairment—often classified as

asymptomatic—who still report movement difficulties, fatigue, or reduced activity. Our current study builds on this work by analyzing the muscle recruitment that underlies the deficits in active goal-directed reaching movements. The outcomes of this work may help develop objective, physiological markers of impaired muscle control that can enhance or surpass existing clinical metrics.

Abnormal muscle recruitment patterns after stroke lead to inappropriate force generation that underlie motor impairment. During reaching, muscle forces serve two primary functions: (1) supporting the arm against gravity—primarily mediated by proximal muscles that span the shoulder and elbow, and (2) compensating for complex limb dynamics—including inertial, Coriolis, and centrifugal forces—primarily mediated by distal muscles that span the elbow and wrist. Muscle forces also generate stiffness and viscosity that help stabilize joints and respond to unexpected perturbations—features that are not fully captured by muscle torques alone. Muscle forces result from muscle contractions caused by motoneuron firing, which is observable with EMG. In our previous work, we demonstrated that the tonic component of EMG reflects muscle forces related to gravity compensation during reaching, while the phasic component reflects the remainder forces related to intersegmental dynamics.[15] After stroke, efforts to actively support the arm against gravity or to load the shoulder often result in coupled elbow moments, which reduce the reachable workspace and restrict movement range.[16–19] This pattern suggests that neural mechanisms for gravity compensation—likely mediated by the reticulospinal system—may become abnormally engaged after stroke.[20–22] In addition, stroke disrupts complex intralimb coordination and grasping[6,17,23], functions that may depend on plasticity within corticospinal projections.[24–26] The reticulospinal and corticospinal systems are

hierarchically organized and anatomically coupled,[27–29] further complicating efforts to develop targeted interventions. In this cross-sectional feasibility study, we investigate how stroke affects the neural motor control mechanisms by testing two hypotheses: 1) stroke affects the recruitment of distal muscles that move the wrist and hand more than proximal and biarticular muscles that move the shoulder and elbow; 2) stroke affects the phasic component of muscle recruitment responsible for gravity compensation more than the tonic component of muscle recruitment responsible for intersegmental dynamics. Testing these hypotheses will result in clinically meaningful insights into post-stroke recovery and provide a foundation for individualized motor rehabilitation approaches.

Methods

Data Collection

The study protocol was approved by West Virginia University's Institutional Review Board (Protocol #1311129283). Participants were recruited from Morgantown, WV area between 2014 and 2017. All participants came provided written informed consent. Participants were grouped as Control and Stroke. The Control group included nine healthy, right-hand dominant individuals (mean age ± SD = 22.78 ± 0.67 years; 3 females, 6 males). Control group inclusion criterion was the age between 18 and 85. The Stroke group included eight individuals (mean age ± SD = 58 ± 6.9 years; 1 female, 7 males) with single unilateral ischemic strokes affecting the middle cerebral artery (n=4, MCA), basal ganglia (n=2, BG), and brainstem (n=2, BS; Table 1). The additional Stroke group inclusion criterion was the diagnosis of stroke in medical records. The exclusion criteria for both groups were 1) pregnancy or breast feeding and 2) medical condition or trauma

that could affect motor performance (other than stroke). Three stroke participants were in the sub-acute phase (<6 months post-stroke), and the rest were chronic (>6 months). The numerical categories assigned to stroke participants reflect their motor deficit level, determined by the dynamic performance index; higher indices represent less severe deficits (Table 1).[4]

Table 1. Characteristics of individuals with stroke.

	Sex	Stroke hemi.	Years after stroke	Age	Performance Index: Gravity	Performance Index: Dynamic	Stroke location details
MCA1	M	right	6	60	4.12 ± 2.30	6.39 ± 0.53	right MCA
MCA2	M	left	0.5	53	2.71 ± 2.11	5.58 ± 0.53	left MCA
MCA3	F	left	3	51	3.47 ± 1.24	4.94 ± 0.14	left MCA
MCA4	M	right	7	53	3.10 ± 1.45	3.99 ± 0.21	Right MCA extending posteriorly
BG1	M	left	5	58	3.85 ± 1.39	5.21 ± 0.30	left caudate lenticular nucleus and external horn of the left ventricle (BG)
BG5	M	right	0.25	68	0.98 ± 0.08	1.27 ± 0.05	lacunar infarct in posterior right putamen and border of right internal capsule (BG)
BS1	M	right	8	51	2.59 ± 2.25	6.57 ± 0.91	right lateral medullary infarction with occluded right vertebral artery (BS)
BS4	M	right	0.5	67	2.79 ± 1.33	3.55 ± 0.45	right dorsal pontine-medullary lacunar infarction (BS)

*MCA, middle cerebral artery; BS, brainstem; BG, basal ganglia; hemi is short for hemisphere.

Participants performed experiments at the NeuroEngineering and Rehabilitation Laboratory at West Vrignia University located in Morgantown, WV during one 2- to 3-hour session scheduled between 2014 and 2017. Participants were asked to reach in virtual reality (VR) shown in 3D environment created with Vizard (Worldviz) and shown via a head-mounted display (Oculus Rift), detailed in earlier publications.[4,15] Briefly, seated participants reached to virtual targets (spheres of 10-cm diameter) displayed at random locations equidistant from a starting position, similar to a standard center-out reaching task. The starting position was adjusted such that each participant's upper arm was aligned with their trunk and forearm was parallel to the floor with palm down (shoulder at 0°, elbow at 90°, wrist at 0° pronated; Fig. 1A). The arm was visualized in VR as a stick figure using motion capture (Impulse system by PhaseSpace Inc) and updated at 90 Hz. Large target size reduced task difficulty, accommodating moderately impaired stroke participants. Target distance was scaled to 30% of each participant's arm length (average 20 cm), except for one severely impaired participant from the Stroke group whose paretic arm reach was reduced to 10 cm.

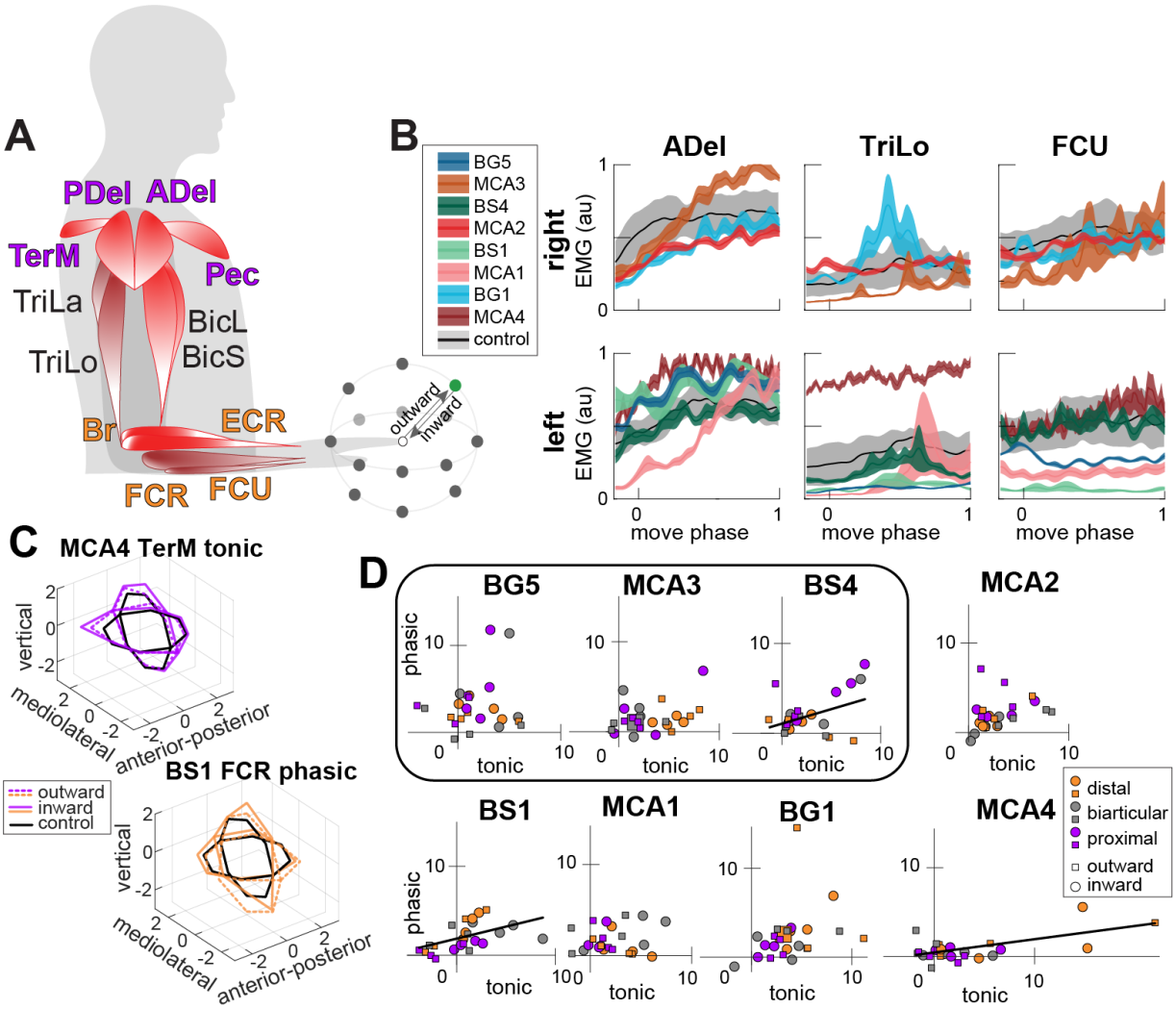

Figure 1. A. Experimental task side view. Each reaching movement was between the central target (open circle) and one of the peripheral targets (outward and inward reaches, green circle shows the exemplar reaching direction), target locations not to scale. Muscle activity was recorded from proximal muscles (purple labels): pectoralis (Pec), teres major (TerM), anterior deltoid (ADel), posterior deltoid (PDel), biarticular muscles (black labels): the long and lateral heads of triceps (TriLo and TriLa), the short and long heads of biceps (BiS and BiL), and distal muscles (orange labels): brachioradialis (Brd), flexor carpi radialis (FCR), flexor carpi ulnaris (FCU), and extensor capri radialis (ECR). Bright red muscles support the arm against gravity in this task; darker-shaded muscles produce force in the direction of gravity. **B**. Examples of filtered and normalized muscle activity profiles for three muscles, abbreviated as in **A**, during outward reach to the green target in **A**. The gray shaded area shows the Control variance, and colors show the mean (line) and standard error (shaded area) for individual participants from the Stroke group. **C.** Plots show examples of tonic (top left) and phasic (bottom right) hemiparetic score differences (color lines) relative to controls (black lines) per reaching direction. The data were used to calculate the areas of the illustrated ellipses termed score tunings. **D.** Plots show tonic vs. phasic hemiparetic score tunings calculated

from data shown in **C** per individual with stroke. The rounded rectangle outlines data for subacute participants. Squares indicate outward and circles indicate inward reaches; the color indicates values summed across proximal, biarticular, or distal muscles. Lines show significant ($p < 0.05$) linear regressions.

During reaching movements, motion capture data was recorded at 480 Hz and surface electromyography (EMG) was recorded at 2,000 Hz using MA400-28 (MotionLab Systems); both datasets were synchronized offline. EMG of twelve muscles was recorded including the clavicular head of pectoralis (Pec), teres major (TerM), anterior deltoid (ADel), posterior deltoid (PDel), the long and lateral heads of triceps (TriLo and TriLa), the short and long heads of biceps (BiS and BiL), brachioradialis (Br), flexor carpi radialis (FCR), flexor carpi ulnaris (FCU), and extensor carpi radialis (ECR, Fig. 1A). EMG data was analyzed in MATLAB (MathWorks Inc). The EMG data recorded from the Control group was reported by Olesh et al. 2017.[15] The kinematic and force data from the Stroke group was reported by Thomas et al. 2021.[4]

Theory

The rotational motion of a joint with a single degree of freedom (DOF), driven by muscle-generated forces acting across the joint, is described by the following equation:

$$I\ddot{\theta} = \tau_m(\theta, \dot{\theta}, a) + \tau_{int}(\dot{\theta}, \theta) + \tau_g(\theta)\ , \qquad \text{(Eq. 1)}$$

where I is the inertia matrix of the body segment attached to the joint, $\theta, \dot{\theta}, \text{and } \ddot{\theta}$ are angle, angular velocity and acceleration of the corresponding DOF, respectively; τ_m are active muscle torques; a is the muscle activation produced by motoneuron firing; τ_{int} is a sum of intrinsic torques due to the interaction of connected segments and other reaction torques from co-contraction or joint viscoelastic properties; and $\tau_g(\theta)$ is a gravitational torque. Only muscle torques are directly controlled by the nervous system.

Therefore, by rearranging Equation (1), we see that to generate appropriate motor output, the nervous system must estimate and account for both body dynamics and external forces as part of the outgoing motor command.

$$\tau_m = I\ddot{\theta} - \tau_{int}(\theta, \dot{\theta}) - \tau_g(\theta) = \tau_d(\ddot{\theta}, \theta, \dot{\theta}) + \left(-\tau_g(\theta)\right), \qquad \text{(Eq. 2)}$$

where τ_d is a lumped parameter for the sum of all torques other than gravity and $-\tau_g(\theta)$ is the anti-gravity torque that the muscles must produce to support the arm against gravity during reaching.

The profile of the muscle torque ($\tau_m^i(t)$) acting about the ith DOF is determined by the product of all muscle forces (F_m(t)) generated by multiple muscles spanning the joint and their respective moment arms (r_m^i). This relationship can be expressed as:

$$\tau_m^i(t) = \sum_{m=1}^{M} r_m^i(\theta_i) \times F_m(t)\ , \qquad \text{(Eq. 3)}$$

where the magnitude and sign of the moment arm $r_m^i(\theta_i)$ indicates the amplitude and direction of muscle moments, defining the agonistic or antagonistic actions of different muscles and their relative importance. The opposing moments produced by antagonistic muscles also contribute to the increased joint stiffness and can be a measure of joint stabilization that may be used to assess muscle fatigue. Equation 3 is a system of equations, one for each DOF, illustrating that every muscle contributes to muscle torques across multiple joints and DOFs.

The relationship between the temporal profile of muscle force $F_m(t)$ and neural activation $a_m(t)$ observable with EMG can then be expressed using Hill-type formulation:[30,31]

$$F_m(\mathrm{t}) = F_{max} f_l\left(l_m(t)\right) f_v\left(\dot{l}_m(t)\right) a_m(t) + f_p\left(l_m(t)\right) \propto \Phi\left(a_m(t)\right), \qquad \text{(Eq. 4)}$$

where F_{max} is the subject-specific maximal isometric force at muscle rest length, $f_l(l_m(t))\, f_v\left(\dot{l}_m(t)\right)$ are intrinsic force-length-velocity relationships that depend on the profile of muscle length $l_m(t)$ and its rate of change $\dot{l}_m(t)$, and $f_p(l_m)$ is the passive tissue forces; all of which can be collapsed into a nonlinear function Φ that is proportional to muscle force. If the neural command to the muscles also embeds the compensation for gravity $a_g(t)$ and intersegmental dynamics $a_d(t)$ and substituting parameters in Equation 1 with those from Equation 2 and 3 we obtain

$$\tau_d(t) \propto \sum_{n=1}^{M} \Phi\big(a_d(t)\big), \qquad \text{(Eq. 4)}$$

$$\tau_g(t) \propto \sum_{n=1}^{M} \Phi\left(a_g(t)\right), \qquad \text{(Eq. 5)}$$

The Equations 4 and 5 show that the muscle recruitment can be related to biomechanical features, such as forces needed to support the arm against gravity and compensate for intersegmental dynamics. In our earlier work we have shown that the tonic and phasic components of EMG are related to the gravitational and dynamic components of muscle torque, respectively.[32] The following analysis examines how these two components of EMG change after stroke.

Data Analysis

EMG recordings were filtered (low-pass at 500 Hz, high-pass at 20 Hz, bandpass at 59-61 Hz), rectified, and further low-pass filtered at 10 Hz following SENIAM guidelines. EMG envelopes were normalized to movement duration, downsampled to 100 samples, and averaged across 15 repetitions per reaching direction for each muscle (total of 336 profiles). The sample size of 15 repetitions was derived empirically, it resulted in inter-trial variability in joint angle measurements of about 5 degrees.[33] EMG amplitudes were

223 scaled using maximum contraction values obtained across all reaching directions (Fig.
224 1B).

225 Principal component analysis (PCA) was used to separate tonic and phasic EMG
226 components. Normalized, demeaned EMG profiles (12 muscles × 14 directions ×
227 inward/outward) were arranged into matrices (An×m; n = 100, m = 336). PCA
228 assumptions for normality (Shapiro-Wilk test) and orthogonality (dot product calculation)
229 were met, while homogeneity (Levene's test) was not, indicating unequal variance across
230 muscles and directions.

231 PCA utilized MATLAB's singular value decomposition, extracting eigenvectors
232 (principal components), variance accounted for (VAF), and scores. PCA was applied
233 separately to data from Control and Stroke groups' left and right arms (Control: left n=9,
234 right n=9; Stroke: left paretic n=5, right paretic n=3, left non-paretic n=3, right non-paretic
235 n=5).

236 Previous studies established that the first eigenvector represents tonic (gravity-
237 related) EMG activity, while the second eigenvector captures phasic (intersegmental
238 dynamic-related) EMG activity,[32] both potentially altered by stroke. PCA scores quantify
239 representation differences of EMG features across reaching directions and muscles. Due
240 to minimal differences,[34] Control scores from left and right arms were combined to
241 enhance normative variability estimate. Paretic scores were then adjusted by subtracting
242 bilateral control scores, measuring stroke-related deficits.

243 Score differences across reaching directions indicate feature recruitment variability
244 dictated by task demands. The elliptical areas defined by these score differences, relative

245 to controls, were calculated (Fig. 1C), providing quantitative measures of muscle over- or
246 under-recruitment in stroke participants for tonic and phasic components.

247 **Statistics and Reproducibility**

248 To determine the impact of stroke on the temporal evolution of the tonic and phasic
249 biomechanical features in EMG, the first 2 eigenvectors and their VAF were compared
250 between bilateral control data and the paretic and non-paretic data from Stroke group.
251 We used the maximal coefficient of determination obtained from cross-correlation
252 (*crosscorr* function in MATLAB Signal Processing Toolbox) between the mean control
253 profile and the non-paretic or paretic individual profile for the 1st and 2nd eigenvector
254 separately.

255 During reaching in certain directions, some muscles may have low tonic and phasic
256 EMG, which would result in low PCA score values. Moreover, stroke can also cause
257 reduced tonic and phasic EMG, which would also result in low scores. Here, we defined
258 low scores as values below 5% of the maximal score. To evaluate the effect of stroke on
259 score amplitude, we performed 2 two-sample t-tests comparing low scores of Control and
260 Stroke groups for tonic and phasic components separately. The familywise error adjusted
261 alpha was equal to 0.0253 using Bonferroni-Sidak correction.

262 We hypothesized that 1) stroke affects the recruitment of distal muscles that move
263 the wrist and hand more than proximal and biarticular muscles that move the shoulder
264 and elbow; 2) stroke affects the phasic component of EMG more than the tonic
265 component. To test these hypotheses, we fitted a non-parametric generalized linear
266 mixed-effects (GLME) model (*fitglme* function in Statistics and Machine Learning Toolbox,
267 MATLAB) with an identity link and normal error distribution to examine the effects of three

continuous predictors—Component (Tonic vs. Phasic), Direction (Outward vs. Inward), and Muscle Group (Proximal, Biarticular, vs. Distal)—on the sum of score tunings, along with their interactions. One-sample Kolmogorov-Smirnov test was performed on the GLME model residuals to check that the normality assumption is not violated (alpha = 0.05; p = 0.58). Random effects variance components were estimated for the intercept across subjects and for the residual error. The table below shows beta coefficients (β) that represent the estimated effects of predictors (fixed effects) on the outcome variable, adjusted for the random effects structure in the model and the associated standard error (SE), confidence intervals (CI), and p-values. The hypotheses will be rejected if the beta values are insignificant at alpha = 0.05.

To test if stroke affects both tonic and phasic EMG in individual participants, we regressed tonic vs. phasic score tunings using linear regression analysis (*regress* function in MATLAB Statistics and Machine Learning Toolbox). We excluded outliers in a percentile threshold from 2.5% to 97.5% (*isoutlier* function in MATLAB Data Preprocessing Toolbox).

To evaluate how stroke deficits measured from joint moments in our earlier study are related to the EMG deficits, we regressed the score tunings for tonic and phasic components during outward and inward reaches against gravitational and dynamic torque performance index. We have also regressed the score tunings against the years since the stroke.

The hemiparetic score values change across reaching directions in proportion to how much a given muscle is over- or under-recruited for a given movement. To determine whether these abnormal recruitment patterns are similar across muscles, we regressed the hemiparetic score differences for 28 reaching directions between each muscle pair

291 for tonic and phasic EMG components separately. We excluded outliers that is more than
292 three median absolute deviations from the median (*isoutlier* function in MATLAB Data
293 Preprocessing Toolbox). This was achieved with linear regression analysis for Control
294 and paretic arm Stroke Groups with adjusted alpha = 0.0008 (Bonferroni-Sidak
295 correction). Linear regression analysis was performed using *regress* function in MATLAB
296 Statistics and Machine Learning Toolbox. Each matrix, $\boldsymbol{C}_{n \times m}$, consisted of n = 28 reaching
297 directions by m = 12 muscles per participant for tonic and phasic EMG components.
298 Significant relationships were indicated by moderate and high coefficients of
299 determination (R^2) for each muscle pair. The resulting matrix of R^2 values, represented
300 as heatmaps in Figures 3 and 4, show how many muscles were over- or under-recruited
301 together in each participant. We also preserved the sign of the regression slope to indicate
302 whether the coupled recruitment represents co-contraction (positive sign) or antagonistic
303 activation (negative sign) of the muscle pair.

304 Sensitivity analysis: to evaluate the effect of differences between dominant and
305 non-dominant motor control on the estimate of stroke deficits, the same analyses were
306 applied to hemiparetic scores normalized to matched data from left- or -right arm of control
307 participants. The results were the same.

308 Results

309 We recruited 19 potentially eligible participants, 2 of whom were ineligible due to
310 trauma to the arm (n=1) and the absence of stroke diagnosis in the medical records (n=1).
311 The remaining 17 eligible participants all completed the study and showed consistent
312 motion and joint moment profiles[4,32] but more variable surface EMG profiles (Fig. 1B).[35]

To understand how muscle recruitment changes after a stroke, we compared the features identified by PCA in individuals in the Control and Stroke groups. Our first step was to confirm that the principal components (i.e., eigenvectors) derived from EMG data in both groups are oriented in similar directions. We found that the temporal patterns of both primary features of the Stroke group were similar to the corresponding features in the Control group (Supplemental Fig. S1A), and they captured a similar amount of variance in EMG (Supplemental Fig. S1B). The variance accounted for (VAF) by the first two principal components from EMG of paretic muscles in the Stroke group was equal to 53% ± 13% and 17% ± 5% (mean ± standard deviation across participants) for 1st (tonic) and 2nd (phasic), respectively. The corresponding values for the Control group were 52% ± 7% and 16% ± 5%, respectively, and for the non-paretic arm in the Stroke group were 54% ± 10% and 19% ± 7%, respectively. This implies that the underlying data structure across individuals shares a common pattern of variance. This agrees with subjective observations of clinicians and scientists that the patterns of post-stroke EMG often appear normal despite motor deficits.

Next, we analyzed the principal component scores, where the amplitude reflects how strongly a specific biomechanical feature — related to gravity or intersegmental dynamics — is expressed in a muscle's EMG activity during movement. Low scores indicate that the feature accounts for little variance in the EMG signal for certain muscles and reaching directions, suggesting abnormal recruitment patterns in the hemiparetic arm after stroke. Our data show that, in control participants, 18% ± 7% (mean ± SD across participants) of tonic scores were low, or below 5% of the maximum, compared to 23% ± 9% for the paretic arm of participants with stroke. A two-sample t-test showed no

significant difference between groups in the proportion of low tonic scores, t(24) = -1.31, p = 0.2013. However, the percentage of low tonic hemiparetic scores across individuals increased with time since stroke (Pearson correlation coefficient R = 0.85, p = 0.0068). Moreover, a significantly higher proportion of phasic hemiparetic scores were low (30% ± 6%) compared to controls (24% ± 6%) (two-sample t-test, t(24) = 2.69, p = 0.0127). There was no linear relationship between the percentage of low phasic hemiparetic scores and time since stroke (R = 0.01, p = 0.9812). This suggests that stroke reduces both components of EMG activity, though to varying degrees depending on individual pathophysiology; the phasic component associated with intersegmental dynamics is most affected.

Altered recruitment patterns were also evident across different reaching directions, each requiring varying combinations of forces for arm support against gravity and for reaching toward or away from a target. Consequently, the expression of biomechanical features in a given muscle's EMG signal varied with reaching direction—a directional variability that was clearly observable in hemiparetic score differences after stroke (Supplementary Figs. S2, S3). We captured these differences in muscle recruitment as score tunings (see Methods above). In this analysis, negative tunings indicate a reduced representation of the feature in the hemiparetic EMG or under-recruitment of muscles, while positive tunings indicate an increased representation or over-recruitment of muscles relative to controls. The resulting score tunings were mainly positive with individual variability in the extend of deficit in tonic and phasic recruitment of proximal, biarticular, and distal muscle groups (Fig. 1D). In three participants (BS4, BS1, and MCA4), the phasic and tonic score tunings were correlated. The variation in tonic and

phasic recruitment deficits across individuals indicates that stroke can impair either mechanism independently or both simultaneously. The GLME model showed a significant intercept (β = 3.85, $p < 0.001$), indicating a nonzero baseline value for the muscle recruitment deficits captured by tonic and phasic score tunings. The Component predictor had a significant negative effect (β = -0.54, $p = 0.020$), showing that the phasic EMG scores (2nd principal component) were not surprisingly lower than the tonic EMG scores (1st principal component). The Muscle Group predictor also had a significant negative effect (β = -0.48, $p = 0.005$), meaning distal and biarticular muscles had lower deficits than proximal muscles. The interaction Component × Muscle Group was significant and positive (β = 0.24, $p = 0.027$), implying that the negative effect of Component depends on the level of Muscle Group — the differences between phasic and tonic recruitment is lower in biarticular and distal muscles compared to proximal muscles. Other predictors and interactions were not statistically significant (Table 2). Random effects analysis showed small variability across participants (SD = 0.09), and residual error SD was 0.42. This shows that after stroke, the damaged motor system over-activates many muscles in the hemiparetic arm—particularly for the action to support the limb against gravity—making movements energy-inefficient and likely contributing to fatigue.

Table 2. Results of the non-parametric generalized linear mixed-effects model.

Predictor	**β**	**SE**	**95% CI (Lower, Upper)**	**t**	**df**	***p*-value**
Intercept	3.849	0.363	[3.128, 4.570]	10.61	88	<.001
Component	-0.541	0.229	[-0.995, -0.087]	-2.37	88	.020
Direction	0.210	0.361	[-0.508, 0.928]	0.58	88	.562
Muscle Group	-0.478	0.168	[-0.810, -0.145]	-2.86	88	.005
Component × Direction	-0.086	0.229	[-0.541, 0.368]	-0.38	88	.706

Component × Muscle Group	0.238	0.106	[0.021, 0.449]	2.25	88	.027
Direction × Muscle Group	-0.266	0.168	[-0.599, 0.067]	-1.59	88	.114
Component × Direction × Muscle Group	0.113	0.106	[-0.098, 0.323]	1.07	88	.289

Lower bound adjustment for the main effect, bold values are significant. Based on a linear model with 96 observations. Both Muscle Group and Component were treated as continuous variables. β - beta coefficients representing the estimated effects of predictors on the hemiparetic score area; SE –standard error; t – Student's t distribution value. All *p*-values are two-tailed.

Deficits in tonic muscle recruitment varied with the time since stroke. However, the deficits in tonic recruitment of proximal muscles were markedly different for outward and inward movements (Fig. 2A), indicating different neural control mechanisms for outward reaching and returning retrieval movements. In chronic stroke participants, tonic overactivation of hemiparetic biarticular muscles during outward reaches decreased as the number of years since stroke increased ($R^2 = 0.90$, $p = 0.019$; Fig. 2A). This trend was especially evident in the short head of triceps ($R^2 = 0.30$, $p = 0.027$). Furthermore, the difference in tonic activation between proximal and distal muscles increased with time post-stroke ($R^2 = 0.45$, $p = 0.019$) with differences between outward and inward reaches diminishing (Fig. 2C). This was driven by increasing tonic overactivation of proximal muscles and decreasing tonic overactivation of distal muscles, but each of these regressions with years since stroke were not significant (chronic proximal: $R^2 = 0.16$, $p = 0.245$; chronic distal: $R^2 = 0.35$, $p = 0.070$). In subacute participants, tonic muscle activation showed marked differences between outward and inward reaches. Outward reaches were dominated by proximal over-recruitment, with summed proximal muscle score tunings of 6.70, 11.56, and 25.09 and corresponding distal muscle differences of –2.4, 2.90, and 6.04 for subjects BG5, BS4, and MCA3, respectively. In contrast, inward reaches exhibited more variable deficits in proximal and distal muscle recruitment, with

summed score tunings of 9.29, 6.69, and 20.72 for proximal muscles, and 9.59, 22.66, and 12.36 for distal muscles in the same subacute individuals. Taken together, the data support clinical observations that subacute stroke phase is distinct from the chronic phase. As more time passes after stroke, the tonic over-recruitment of proximal muscle tends to increase or stay the same while the tonic over-recruitment of biarticular and distal muscles tends to decline.

Deficits in phasic muscle recruitment also varied with the time since stroke. The phasic over-activation of distal muscles decreased across all participants ($R^2 = 0.52$, $p = 0.002$; Fig. 2B). These trends were present in flexor carpi radialis ($R^2 = 0.40$, $p = 0.009$) and flexor carpi ulnaris ($R^2 = 0.36$, $p = 0.015$). Moreover, the difference in phasic over-activation between proximal and distal muscles ($R^2 = 0.44$, $p = 0.005$) and between biarticular and distal muscles ($R^2 = 0.46$, $p = 0.004$) also increased with time post-stroke (Fig. 2D). These trends were primarily driven by the progressive decrease in phasic over-recruitment of distal muscles in individuals further removed from the time of stroke onset, consistent with the findings in Fig. 2B. Moreover, the differences between proximal and distal muscles in phasic and tonic activation were correlated across all participants ($R^2 = 0.38$, $p = 0.011$), indicating a similar underlying neural mechanism of decreasing both tonic and phasic over-recruitment of distal muscles. Overall, these results suggest that adaptation over time since stroke is most evident in the reduced activation of distal muscles compare to the activation of proximal and biarticular muscles, especially in the phasic component of muscle recruitment.

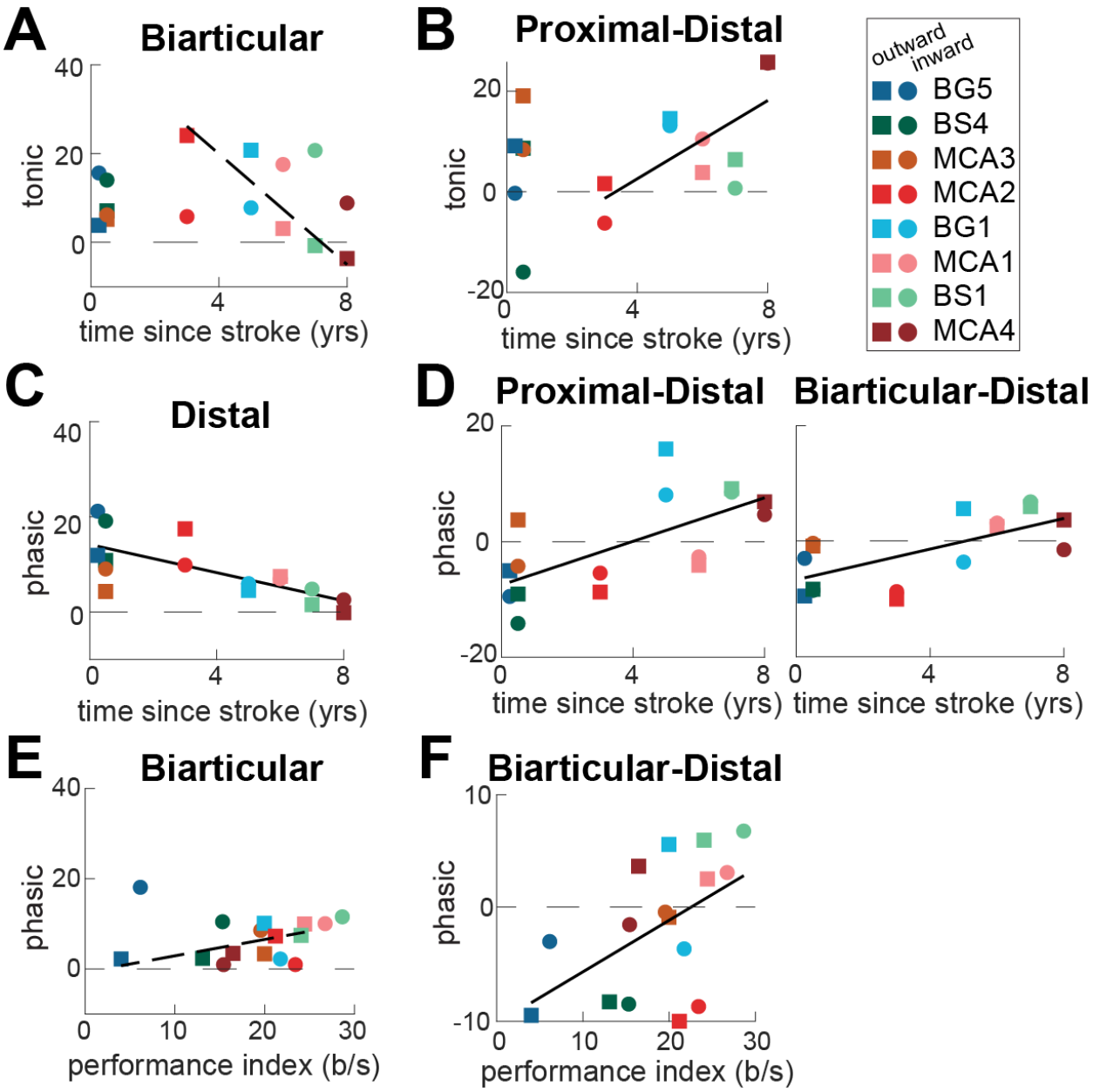

Figure 2. Deficits in muscle recruitment. A. Plot shows tonic score tunings for the biarticular muscles plotted against the number of years post-stroke. Squares indicate outward and circles indicate inward reaches for individual participants; color coded as in Fig. 1. The dashed line shows a significant ($p < 0.05$) linear regression for the outward reaches by chronic participants. **B.** Plot shows tonic score tunings calculated between proximal and distal muscles plotted against the number of years post-stroke, styled as in **A**. The line shows a significant linear regression across all reaching directions by chronic participants. **C.** Plot shows phasic score tunings for the distal muscles plotted against the number of years post-stroke, styled as in **A**. The line shows a significant linear regression across all reaching directions and participants. **D.** Plots show phasic score tunings calculated between proximal and distal (left plot) and biarticular and distal (right plot)

436 muscles plotted against the number of years post-stroke, styled as in **A**. Lines show
437 significant linear regressions across all reaching directions and participants. **E.** Plot shows
438 phasic hemiparetic score tunings for the biarticular muscles plotted against the dynamic
439 performance index, styled as in **A**. The dashed line shows a significant linear regression
440 for the outward reaches by chronic participants. **F.** Plot shows phasic hemiparetic score
441 tunings calculated between biarticular and distal muscles plotted against the dynamic
442 performance index, styled as in **A**. The line shows a significant linear regression across
443 all reaching directions and participants.
444

445 Stroke-induced motor deficits during reaching are reflected in muscle torques,
446 which represent the forces required to move the limb. These torques can be further
447 decomposed into components corresponding to the forces necessary for arm support
448 against gravity and those required to propel the limb during reaching. Given that muscle
449 torques arise from the combined actions of all muscle groups, our EMG analysis enabled
450 quantification of the contributions of specific muscle groups to post-stroke motor
451 impairments. We have shown in an earlier study that the performance index derived from
452 the dynamic component of muscle torques, which is similar to the phasic component of
453 EMG,[15] is a sensitive indicator of the severity of post-stroke motor deficits.[14] Here too we
454 have found that the severity of motor deficits measured with the performance index
455 derived from muscle torques was linearly related to the number of years post-stroke
456 (gravitational performance index vs. years: $R^2 = 0.27$, $p = 0.039$; dynamic performance
457 index vs. years: $R^2 = 0.32$, $p = 0.023$). Moreover, the phasic over-recruitment of biarticular
458 muscles during outward reaches exhibited a strong linear relationship with the summed
459 performance index derived from the dynamic component of shoulder and elbow muscle
460 torques ($R^2 = 0.55$, $p = 0.036$; Fig. 2E). This association was particularly notable in the
461 short head of the biceps ($R^2 = 0.28$, $p = 0.034$) and showed an inverse relationship in the
462 flexor carpi radialis ($R^2 = 0.29$, $p = 0.031$) across both outward and inward reaches.

463 Furthermore, phasic score differences between biarticular and distal muscles were
464 linearly related to the dynamic performance index (R^2 = 0.27, p = 0.038; Fig. 2F).
465 Collectively, these findings demonstrate that stroke-related changes in muscle
466 recruitment patterns directly contribute to impairments in generating the forces necessary
467 for limb propulsion and coordinating movement across joints during reaching tasks.

468 The results above show that post-stroke muscle activation deficits affect entire
469 muscle groups rather than individual muscles. To explore this further, we examined
470 muscle coactivation—that is, the simultaneous recruitment of multiple muscles to perform
471 a given task. The coactivation between antagonistic muscles also contributes to joint or
472 limb stiffness, an important parameter controlled by the central nervous system. In
473 previous work, we showed that in control participants, tonic activity in biarticular and distal
474 muscles, especially in the left arm, was broadly correlated across reaching directions,
475 reflecting their coactivation to support the arm against gravity.[36] However, there was
476 substantial variability across individuals, with two control participants showing few co-
477 activating muscle pairs in the left arm (Fig. 3A). After stroke, the number of tonically co-
478 activating muscle pairs in left-paretic participants was near the lower end of the control
479 range, whereas in right-paretic participants, it was near the upper end (Fig. 3B, C). In
480 contrast, control participants showed minimal phasic coactivation in both arms[36] (Fig. 4A),
481 and this pattern remained largely unchanged after stroke, with few phasically co-
482 activating muscle pairs observed (Fig. 4B, C). Notably, we found a significant inverse
483 linear relationship between the number of phasically co-activating proximal and distal
484 muscles and the dynamic performance index (R^2 = 0.67, p = 0.013), indicating that greater

impairments in generating propulsive forces are associated with more abnormal coactivation between proximal and distal muscles.

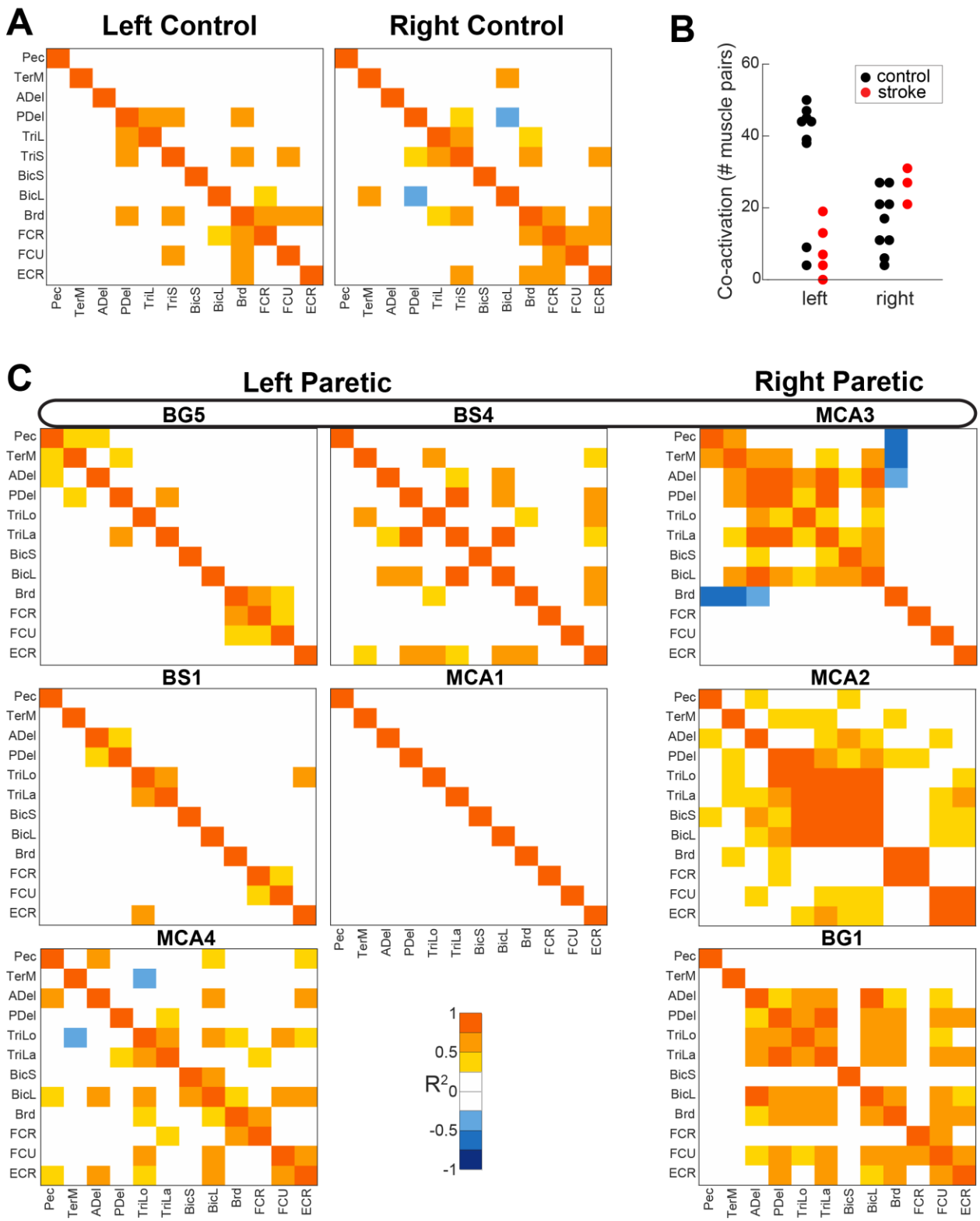

Figure 3. Tonic coactivation. A. Heatmaps show matrices of significant regressions between tonic scores of muscle pairs across reaching directions with the left (left plot) and right (right plot) limb by a young control participant (S5 from Korol et al. 2025) who showed fewer coactivations between muscles of their left arm. The colors show the values of the coefficient of determination (R^2) for regressions between the tonic scores of muscle pairs across reaches in multiple directions. **B.** Symbols show the number of moderate and strong (R^2 >0.5) muscle coactivations in individuals with (red) and without (black) stroke. **C.** Heatmaps of tonic muscle coactivations for participants with stroke during reaching with their paretic arm. Colors are as in **A**.

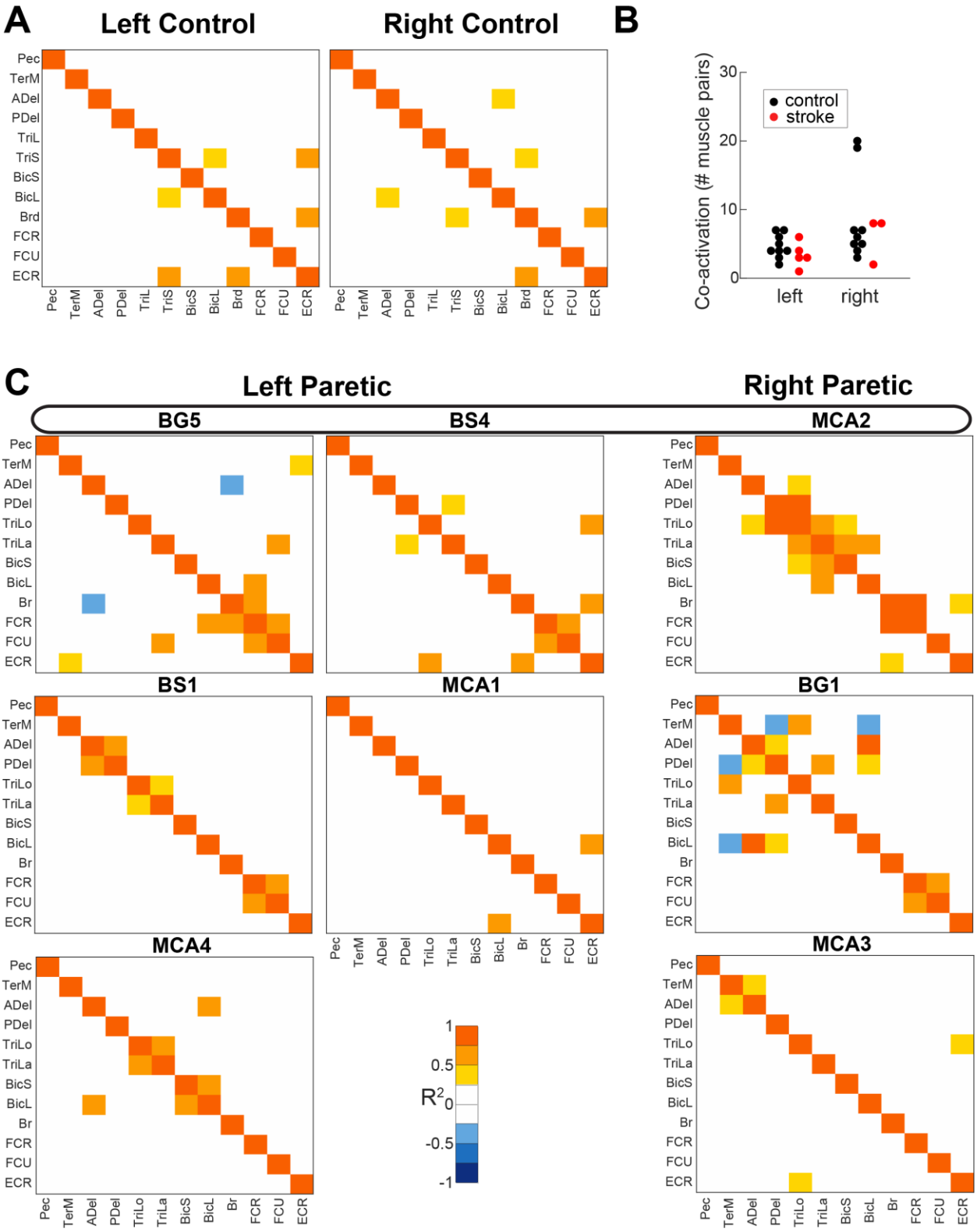
A
Left Control
Right Control
B
Co-activation (# muscle pairs)
control
stroke
left
right
C
Left Paretic
Right Paretic
BG5
BS4
MCA2
BS1
MCA1
BG1
MCA4
MCA3
Pec
TerM
ADel
PDel
TriL
TriS
BicS
BicL
Brd
FCR
FCU
ECR
TriLo
TriLa
Br
R2

Figure 4. Phasic coactivation. A. Heatmaps show matrices of significant regressions between phasic scores of muscle pairs across reaching directions with the left (left plot) and right (right plot) limb by a young control participant (S5 from Korol et al. 2025). The colors show the value of the coefficient of determination (R^2) for regressions between the phasic scores of muscle pairs across reaches in multiple directions. **B.** Symbols show the number of moderate and strong (R^2 >0.5) muscle coactivations in individuals with (red) and without (black) stroke. **C.** Heatmaps of phasic muscle coactivations for participants with stroke during reaching with their paretic arm. Colors are as in **A**.

Discussion

Our results show that stroke disrupts muscle recruitment during reaching, even among individuals with mild impairments. Distal muscle impairment severity increases over time post-stroke, but proximal muscles are also abnormally over-recruited during movements that usually require less activation, indicating disrupted directional tuning. Additionally, paretic muscle coactivation between proximal and distal muscles is abnormal. These findings reject the hypothesis that stroke primarily impacts distal muscles more severely than proximal or biarticular muscles, as both groups are variably affected.

Our results further reject the hypothesis that stroke disproportionately affects the phasic component of EMG compared to the tonic component. Instead, deficits in phasic and tonic recruitment correlate linearly in some participants, and phasic and tonic differences between proximal and distal recruitment correlate across participants and align with overall reaching impairments. This suggests that stroke prompts widespread muscle over-activation, particularly for supporting the limb against gravity, resulting in inefficient movements and potential fatigue.

Our data clarify how stroke damages specific neural control pathways, influencing motor impairment and recovery. Our results suggest that the natural organization of

526 muscles into proximal and distal groups,[37] is differentially impacted by stroke. This may
527 be caused by the individual stroke-related damage to the reticulospinal pathways that
528 contributes to abnormal flexor synergies and over-engagement of proximal muscles[20,46]
529 and to the corticospinal pathway that governs distal fine motor control.[43] The limitation of
530 this conclusion is the small sample size of the study. Power analysis (MATLAB function
531 *sampsizepwr*) indicates that to detect the mean change of 0.478 ± 1.027 SD in post-stroke
532 recruitment between muscle groups (Table 1) with 80% power, the study needs 30
533 participants with stroke. Future studies with this sample sizes will reveal the details of how
534 the plasticity in the two pathways affect muscle recruitment after stroke.

535 Identifying underlying causes of movement inefficiency and fatigue remains
536 challenging, but assessing mechanical impedance provides a quantitative framework.[47]
537 Impedance, comprising stiffness and viscosity, increases during unstable tasks or when
538 precision is required.[48–50] Our results show that after stroke, lateralization of impedance
539 control is disrupted: right-hemisphere strokes reduce consistent muscle coactivations
540 typical of non-dominant hemisphere-driven gravity compensation,[35] while left-hemisphere
541 strokes increase coactivation. Greater deficits in generating propulsive forces also
542 correlate with abnormal coactivation patterns, underscoring that stroke-induced
543 disruption in impedance control significantly contributes to motor inefficiency and fatigue.
544 Quantifying such disruptions may help pinpoint their underlying neural causes and guide
545 more targeted rehabilitation strategies.

Funding

V.G. was supported by NIGMS grants P20GM109098 and P30GM103503. A.S.K. was supported by a fellowship from NIGMS T32 AG052375. This work was supported in part by the Office of the Assistant Secretary of Defense for Health Affairs through the Restoring Warfighters with Neuromusculoskeletal Injuries Research Program (RESTORE) under Award No. W81XWH-21-1-0138. Opinions, interpretations, conclusions, and recommendations are those of the author and are not necessarily endorsed by the Department of Defense. The funders had no role in study design, data collection and analysis, decision to publish, or preparation of the manuscript.

References

1. Feigin VL, Stark BA, Johnson CO, Roth GA, Bisignano C, Abady GG, Abbasifard M, Abbasi-Kangevari M, Abd-Allah F, Abedi V, et al. Global, regional, and national burden of stroke and its risk factors, 1990–2019: a systematic analysis for the Global Burden of Disease Study 2019. *The Lancet Neurology*. 2021;20:795–820.

2. Langhorne P, Coupar F, Pollock A. Motor recovery after stroke: a systematic review. *The Lancet Neurology*. 2009;8:741–754.

3. Kwakkel G, Kollen BJ, Van Der Grond J, Prevo AJH. Probability of Regaining Dexterity in the Flaccid Upper Limb: Impact of Severity of Paresis and Time Since Onset in Acute Stroke. *Stroke*. 2003;34:2181–2186.

566 4. Thomas AB, Olesh EV, Adcock A, Gritsenko V. Muscle torques and joint accelerations
567 provide more sensitive measures of poststroke movement deficits than joint angles.
568 *Journal of Neurophysiology*. 2021;126:591–606.

569 5. Krakauer JW, Carmichael ST. Broken Movement: The Neurobiology of Motor
570 Recovery After Stroke. MIT Press; 2017.

571 6. Pollock A, Farmer SE, Brady MC, Langhorne P, Mead GE, Mehrholz J, van Wijck F.
572 Interventions for improving upper limb function after stroke. *Cochrane Database Syst*
573 *Rev*. 2014;CD010820.

574 7. Hsieh Y, Wu C, Lin K, Chang Y, Chen C, Liu J. Responsiveness and Validity of Three
575 Outcome Measures of Motor Function After Stroke Rehabilitation. *Stroke*.
576 2009;40:1386–1391.

577 8. van der Lee J, Beckerman H, Lankhorst G, Bouter L. The responsiveness of the Action
578 Research Arm and the Fugl-Meyer Assessment Scale in Chronic Storke Patients.
579 *Journal of Rehabilitation Medicine*. 2001;33:110–113.

580 9. Duncan P, Studenski S, Richards L, Gollub S, Lai SM, Reker D, Perera S, Yates J,
581 Koch V, Rigler S, et al. Randomized Clinical Trial of Therapeutic Exercise in
582 Subacute Stroke. *Stroke*. 2003;34:2173–2180.

583 10. Saposnik G, Cohen LG, Mamdani M, Pooyania S, Ploughman M, Cheung D, Shaw
584 J, Hall J, Nord P, Dukelow S, et al. Efficacy and safety of non-immersive virtual reality
585 exercising in stroke rehabilitation (EVREST): a randomised, multicentre, single-blind,
586 controlled trial. *Lancet Neurol*. 2016;15:1019–1027.

11. Wolf SL, Thompson PA, Winstein CJ, Miller JP, Blanton SR, Nichols-Larsen DS, Morris DM, Uswatte G, Taub E, Light KE, et al. The EXCITE stroke trial: comparing early and delayed constraint-induced movement therapy. *Stroke*. 2010;41:2309–2315.

12. Olesh EV, Yakovenko S, Gritsenko V. Automated Assessment of Upper Extremity Movement Impairment due to Stroke. *PLoS ONE*. 2014;9:e104487.

13. Gritsenko V, Dailey E, Kyle N, Taylor M, Whittacre S, Swisher AK. Feasibility of Using Low-Cost Motion Capture for Automated Screening of Shoulder Motion Limitation after Breast Cancer Surgery. *PLoS ONE*. 2015;10:e0128809.

14. Thomas AB, Olesh EV, Adcock A, Gritsenko V. Muscle torques and joint accelerations provide more sensitive measures of poststroke movement deficits than joint angles. *J Neurophysiol*. 2021;126:591–606.

15. Olesh EV, Pollard BS, Gritsenko V. Gravitational and Dynamic Components of Muscle Torque Underlie Tonic and Phasic Muscle Activity during Goal-Directed Reaching. *Frontiers in Human Neuroscience* [Internet]. 2017 [cited 2023 Mar 16];11. Available from: https://www.frontiersin.org/articles/10.3389/fnhum.2017.00474

16. Beer RF, Ellis MD, Holubar BG, Dewald JPA. Impact of gravity loading on post-stroke reaching and its relationship to weakness. *Muscle Nerve*. 2007;36:242–250.

17. Beer RF, Dewald JPA, Dawson ML, Rymer WZ. Target-dependent differences between free and constrained arm movements in chronic hemiparesis. *Experimental Brain Research*. 2004;156:458–470.

608 18. Dewald JPA, Pope PS, Given JD, Buchanan TS, Rymer WZ. Abnormal muscle
609 coactivation patterns during isometric torque generation at the elbow and shoulder
610 in hemiparetic subjects. *Brain*. 1995;118:495–510.

611 19. Sukal TM, Ellis MD, Dewald JPA. Shoulder abduction-induced reductions in reaching
612 work area following hemiparetic stroke: neuroscientific implications. *Exp Brain Res*.
613 2007;183:215–223.

614 20. Ellis MD, Drogos J, Carmona C, Keller T, Dewald JPA. Neck rotation modulates
615 flexion synergy torques, indicating an ipsilateral reticulospinal source for impairment
616 in stroke. *Journal of Neurophysiology*. 2012;108:3096–3104.

617 21. McPherson JG, Chen A, Ellis MD, Yao J, Heckman CJ, Dewald JPA. Progressive
618 recruitment of contralesional cortico-reticulospinal pathways drives motor
619 impairment post stroke. *The Journal of Physiology*. 2018;596:1211–1225.

620 22. Riddle CN, Edgley SA, Baker SN. Direct and Indirect Connections with Upper Limb
621 Motoneurons from the Primate Reticulospinal Tract. *J. Neurosci.* 2009;29:4993–
622 4999.

623 23. Beer RF, Dewald JPA, Rymer WZ. Deficits in the coordination of multijoint arm
624 movements in patients with hemiparesis: evidence for disturbed control of limb
625 dynamics. *Experimental Brain Research*. 2000;131:305–319.

626 24. Gritsenko V, Kalaska JF, Cisek P. Descending Corticospinal Control of
627 Intersegmental Dynamics. *Journal of Neuroscience*. 2011;31:11968–11979.

25. Gribble PL, Ostry DJ. Compensation for Interaction Torques During Single- and Multijoint Limb Movement. *Journal of Neurophysiology*. 1999;82:2310–2326.

26. Liepert J, Bauder H, Miltner WHR, Taub E, Weiller C. Treatment-Induced Cortical Reorganization After Stroke in Humans. *Stroke*. 2000;31:1210–1216.

27. Baker SN. The primate reticulospinal tract, hand function and functional recovery. *The Journal of Physiology*. 2011;589:5603–5612.

28. Baker SN, Perez MA. Reticulospinal Contributions to Gross Hand Function after Human Spinal Cord Injury. *J. Neurosci.* 2017;37:9778–9784.

29. Glover IS, Baker SN. Both Corticospinal and Reticulospinal Tracts Control Force of Contraction. *J. Neurosci.* 2022;42:3150–3164.

30. Hill AV. Recovery Heat in Muscle. *Proceedings of the Royal Society of London. Series B, Biological Sciences*. 1939;127:297–307.

31. Hill AV. The heat of shortening and the dynamic constants of muscle. *Proceedings of the Royal Society of London. Series B - Biological Sciences*. 1938;126:136–195.

32. Olesh EV, Pollard BS, Gritsenko V. Gravitational and Dynamic Components of Muscle Torque Underlie Tonic and Phasic Muscle Activity during Goal-Directed Reaching. *Front Hum Neurosci*. 2017;11:474.

33. Bahdasariants S, Yough MG, Gritsenko V. Impedance-based biomechanical method for robust inverse kinematics from noisy data. *IEEE Sens. Lett.* 2024;8:1–4.

34. Korol A, Gritsenko V. Differential Impact of Biomechanical Constraints on Control Signal Dimensionality for Gravity Support Versus Propulsion [Internet]. 2024 [cited 2024 May 13];Available from: http://biorxiv.org/lookup/doi/10.1101/2024.02.12.579990

35. Korol AS, Gritsenko V. Control signal dimensionality depends on limb dynamics. *PLOS ONE*. 2025;20:e0322092.

36. Korol AS, Gritsenko V. Control signal dimensionality depends on limb dynamics. *PLOS ONE*. 2025;20:e0322092.

37. Gritsenko V, Hardesty RL, Boots MT, Yakovenko S. Biomechanical Constraints Underlying Motor Primitives Derived from the Musculoskeletal Anatomy of the Human Arm. *PLoS ONE*. 2016;11:e0164050.

38. Taitano RI, Yakovenko S, Gritsenko V. Neuromechanical Coupling is Reflected in the Spatial Organization of the Spinal Motoneuron Pools [Internet]. West Virginia University; 2022 [cited 2022 Dec 8]. Available from: http://biorxiv.org/lookup/doi/10.1101/2022.07.09.499432

39. Yakovenko S, Mushahwar V, VanderHorst V, Holstege G, Prochazka A. Spatiotemporal Activation of Lumbosacral Motoneurons in the Locomotor Step Cycle. *Journal of Neurophysiology*. 2002;87:1542–1553.

40. Toossi A, Bergin B, Marefatallah M, Parhizi B, Tyreman N, Everaert DG, Rezaei S, Seres P, Gatenby JC, Perlmutter SI, et al. Comparative neuroanatomy of the

667 lumbosacral spinal cord of the rat, cat, pig, monkey, and human. *Sci Rep*.
668 2021;11:1955.

669 41. Penfield W, Rasmussen T. The cerebral cortex of man: A Clinical Study of
670 Localization of Function. 1950.

671 42. Wassermann EM, McShane LM, Hallett M, Cohen LG. Noninvasive mapping of
672 muscle representations in human motor cortex. *Electroencephalography and Clinical*
673 *Neurophysiology/ Evoked Potentials*. 1992;

674 43. Lawrence DG, Kuypers HG. The functional organization of the motor system in the
675 monkey. I. The effects of bilateral pyramidal lesions. *Brain : a journal of neurology*.
676 1968;91:1–14.

677 44. Hardesty RL, Ellaway PH, Gritsenko V. The Human Motor Cortex Contributes to
678 Gravity Compensation to Maintain Posture and During Reaching. *Journal of*
679 *Neurophysiology*. 2023;129:83–101.

680 45. Schieppati M, Trompetto C, Abbruzzese G. Selective facilitation of responses to
681 cortical stimulation of proximal and distal arm muscles by precision tasks in man.
682 *Journal of Physiology*. 1996;491:551–562.

683 46. Ellis MD, Acosta AM, Yao J, Dewald JPA. Position-dependent torque coupling and
684 associated muscle activation in the hemiparetic upper extremity. *Exp Brain Res*.
685 2007;176:594–602.

686 47. Mizrahi J. Mechanical Impedance and Its Relations to Motor Control, Limb
687 Dynamics, and Motion Biomechanics. *J. Med. Biol. Eng.* 2015;35:1–20.

688 48. Rancourt D, Hogan N. Stability in force-production tasks. *Journal of Motor Behavior*.
689 2001;

690 49. Milner TE. Adaptation to destabilizing dynamics by means of muscle cocontraction.
691 *Experimental Brain Research*. 2002;

692 50. Burdet E, Osu R, Franklin DW, Milner TE, Kawato M. The central nervous system
693 stabilizes unstable dynamics by learning optimal impedance. *Nature*. 2001;414:446–
694 449.

695